Chinese Chemical Letters 35 (2024) 108823

Contents lists available at ScienceDirect

Chinese Chemical Letters

journal homepage: www.elsevier.com/locate/cclet

Förster resonance energy transfer reveals phillygenin and swertiamarin concurrently target AKT on different binding domains to increase the anti-inflammatory effect

Xiaoyao Ma[a,b,1], Jinling Zhang[a,1], Ge Fang[a], He Gao[a], Jie Gao[a,*], Li Fu[c,*], Yuanyuan Hou[a,*], Gang Bai[a]

[a] State Key Laboratory of Medicinal Chemical Biology, College of Pharmacy and Tianjin Key Laboratory of Molecular Drug Research, Nankai University, Tianjin 300000, China
[b] College of Life Health, Dalian University, Dalian 116622, China
[c] Dalian Fusheng Pharmaceutical Co., Ltd., Dalian 116000, China

ARTICLE INFO

Article history:
Received 26 April 2023
Revised 11 July 2023
Accepted 18 July 2023
Available online 21 July 2023

Keywords:
FRET
Swertiamarin
Phillygenin
AKT
Anti-inflammation
Combinatorial drug

ABSTRACT

The clinical benefit of combination therapy is significant, but it is not easy to define the mechanism of complexity and diversity. Previous studies illustrate that phillygenin (Phi) binds in the allosteric inhibit pocket of protein kinase B (AKT), and swertiamarin (Swe) acts on the pleckstrin homology (PH) domain of AKT. However, the combined synergistic effect of relieving the inflammatory response has yet to be elucidated. Based on high sensitivity, specificity and fast-responsibility fluorescent sensors, the Förster resonance energy transfer (FRET) technique offers a route to provide clear insights into physiological and pathological processes. In the study, molecular docking, the fluorescent probes of Phi and Swe for FRET were designed and synthesized. FRET analysis shown that Swe and Phi concurrently acted on the PH domain and allosterically inhibited pocket of AKT, respectively. The combination of Swe and Phi significantly increased the heat stability of AKT and decreased protease-induced degeneration. In lipopolysaccharides (LPS)-induced mice and cells, the combination arrested AKT activation, nuclear factor kappa-B (NF-κB) phosphorylation, and the expression of tumor necrosis factor-α (TNF-α), interleukin (IL)-6 and IL-8. In conclusion, FRET revealed Phi and Swe concurrently targeted AKT on different domains and the combination of Phi and Swe enhanced the anti-inflammatory effect.

The combination therapies of the compounds are able to enhance the treatment of disease, such as increasing safety and optimizing efficacious preparations [1]. Moreover, studies have shown that disease resistance is less likely to occur against a combination of compounds than to single active constituents [2]. Amoxicillin and clavulanic acid, a combination of penicillin antibiotics and beta-lactamase inhibition, have been widely used for various infections caused by susceptible bacteria [3,4]. The concept of synergistic effects in natural products has gained attention, for example, cinnamaldehyde promoted the antimelanoma activity of dacarbazine both *in vivo* and *in vitro*. The combination of cinnamaldehyde and dacarbazine enhanced cell cycle arrest in the S phase and significantly inhibited melanoma growth [5]. Epigallocatechin-3-gallate inhibited the expression of adenosine triphosphate (ATP) binding cassette transporter and enhanced the intracellular concentration of 5-fluorouracil (5-FU), which markedly increased growth inhibition of human colon cancer cells and human colon adenocarcinoma cells [6].

In general, the combination of compounds increases the biological effect *via* targeting the same or multiple signaling pathways. Hence, the evaluation of combination effects between active compounds has become an important topic in pharmacology [7,8]. Combinatorial drug therapy is complex and diverse, and revealing the mechanisms is the key for further application. Resveratrol and quercetin synergistically regulated the mitogen-activated protein kinase (MAPK) pathway to inhibit thrombin-induced c-Jun N-terminal kinase (JNK) activation and neutrophil migration in endothelial cells [9]. The combination of pumpkin polysaccharides and puerarin alleviated insulin resistance and exerted cytoprotective effects by affecting the Nrf2 and PI3K/AKT signaling pathways in diabetic mice [10]. Moreover, the combination also synergisti-

* Corresponding authors.
E-mail addresses: gaojie@nankai.edu.cn (J. Gao), 2295957379@qq.com (L. Fu), houyy@nankai.edu.cn (Y. Hou).
[1] These authors contributed equally to this work.

https://doi.org/10.1016/j.cclet.2023.108823
1001-8417/

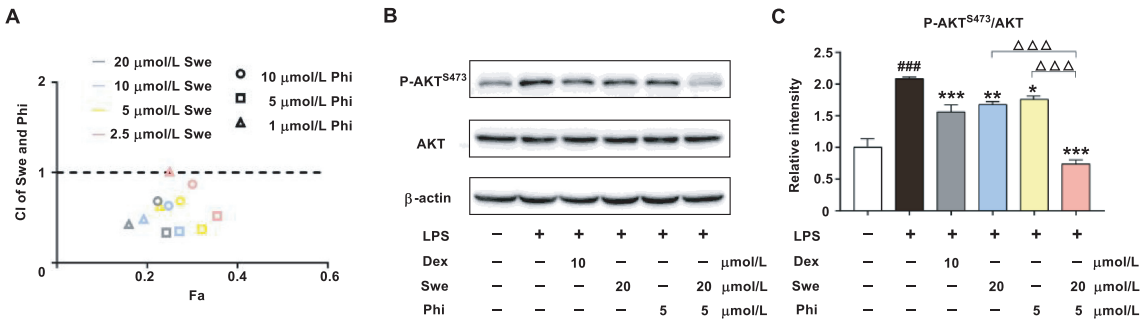

Fig. 1. Screening of the combination dose in cells. (A) CI analysis of different dose combinations of Phi and Swe by the inhibitory effect on NF-κB in TNF-α induced HEK 293 cells. BEAS-2B cells were stimulated with LPS for 30 min with or without pretreatment with Phi, Swe or the combination of Phi and Swe. The activation of AKT was detected by Western blot (B), and the relative intensity of P-AKT^{S473} to that of total AKT is presented as the mean ± standard deviation (SD) of three experiments (C). $^{\#\#\#}P < 0.001$ compared to the control group; $^{*}P < 0.05$, $^{**}P < 0.01$, $^{***}P < 0.001$ compared to the model group (LPS group); $^{\Delta\Delta\Delta}P < 0.001$ compared to the combination group (Swe plus Phi).

cally increased bioactivity by enhancing the bioavailability or uptake of each other, targeting gut microbial profiles and influencing gut integrity [11]. However, it is still challenging to clarify the synergistic mechanism accurately.

Swertiamarin (Swe), a secoiridoid glycoside, is found in the family Gentianaceae. It has been reported to exert various pharmacological effects, including anti-inflammation, antioxidant and liver protection [12]. Phillygenin (Phi) is a lignan component extracted from the fruit of *Forsythia suspensa* with a wide range of bioactivities, such as anti-inflammatory, antitumor and attenuating liver fibrosis effects [13]. Our previous studies illustrated that Swe and Phi both exert anti-inflammatory effects by targeting protein kinase B (AKT) [14,15]. Swe acts on the pleckstrin homology (PH) domain of AKT, and Phi binds in the allosteric inhibit pocket of AKT. By targeting the different binding domains to inhibit AKT, it suggested that Swe and Phi have the potential to combine to block the activation of AKT. However, few studies have analyzed the combination mechanism and revealed the details between Swe and Phi in the process of attenuating inflammation by inhibiting AKT phosphorylation and membrane transport.

Förster resonance energy transfer (FRET) is an energy transfer process between a pair of light-sensitive molecules, where the donor fluorophore, initially in its electronic excited state, transfers energy to an acceptor chromophore [16]. It has been extensively used in various fields, including biological, food safety and biomedical research [17–19]. Based on high sensitivity, specificity and fast-responsibility fluorescent sensors, the FRET technique offers a route to provide clear insights into physiological and pathological processes [20,21]. In particular, FRET-based small-molecule fluorescent probes are often used as photochemical sensors and imaging agents in biological analysis [22]. In combinatorial drug therapy, a FRET-based disulfide-linked xanthene-coumarin-chlorambucil conjugate probe was used successfully for real-time monitoring of drug delivery [23].

To reveal the combination mechanism, in this paper, Phi- and Swe- derived fluorescent probes, Phi-BODIPY@TMR (BTMR) and Swe-BODIPY@TR (BTR), were prepared to analyze the binding condition of Phi and Swe in the structure of AKT by FRET detection *in vitro* and *in vivo*. Subsequently, pathological and biochemical analyses were performed to verify the combined effects of Phi and Swe in a lipopolysaccharides (LPS)-induced inflammation mouse model. The synergistic effect of Phi and Swe inhibiting AKT activity by concurrently targeting the different domains of AKT to alleviate inflammation was finally revealed. The animal experiments were approved by the Animal Ethics Committee, Nankai University (Tianjin, China) and were performed in accordance with the guidelines of the national legislation of China. The use and care of mice for the study described herein was approved (DW20200711-098). The material information and detailed experimental procedures are described in Supporting information.

Firstly, we screened the optimal combination dose of Phi and Swe for anti-inflammatory effects. According to combination index (CI) analysis, the different combinations of Phi and Swe enhanced the inhibitory effect on the expression of nuclear factor kappa-B (NF-κB) (CI < 1), which compared to the same dose of Phi or Swe treatment. The CI of 5 μmol/L Phi combined with 20 μmol/L Swe was the lowest score in all combination doses, which suggested that it was the optimal combination dose to alleviate inflammation (Fig. 1A). In LPS-induced inflammatory BEAS-2B cells, the phosphorylation of AKT significantly increased, and the activation of AKT was markedly decreased by 5 μmol/L Phi or 20 μmol/L Swe as well as the positive drug dexamethasone. Compared to the Phi group and Swe group, the inhibitory effect of the combination observably enhanced AKT activity (Figs. 1B and C). The results suggested that the combination of 5 μmol/L Phi and 20 μmol/L Swe significantly increased the anti-inflammatory effect and the inhibitory effect on AKT activity.

Based on our previous studies, in which both Phi and Swe target AKT to reduce inflammation, molecular docking was performed to provide additional insights into the interactions of AKT with Phi and Swe [14,15]. The top-scoring poses of Phi and Swe were displayed as three dimensional (3D) maps in Fig. 2A. As a result, Phi acted on the allosteric inhibit pocket of AKT, which did not disturb the binding of Swe with the PH domain of AKT. It is known that the FRET efficiency depends on the spectral overlap between the donor fluorescence and the acceptor extinction, and the distance from donor to acceptor, which typically range from less than 100 Å [24]. Fortunately, the distance between Phi and Swe was approximately 14.9 Å to 23 Å (Fig. S1 in Supporting information). Hence, the FRET assay was fit for analyzing whether Phi and Swe concurrently bind to the different domains of AKT protein. The structures and design ideas of the Phi-BTMR and Swe-BTR probes are shown in Figs. 2B and C, and the synthesis route is detailed in Schemes S1 and S2 (Supporting information). The cell counting kit-8 (CCK8) results demonstrated that both Phi-BTMR and Swe-BTR probes did not affect the cell viability in BEAS-2B cells under 100 μmol/L (Fig. S2 in Supporting information). Moreover, the inhibitory effects of Phi-BTMR and Swe-BTR probes on AKT activation were evaluated in LPS-induced BEAS-2B inflammatory cells (Fig. S3 in Supporting information). Due to the similar effects, Phi-BTMR and Swe-BTR probes were suggested to replace prototype drugs for subsequent localization analysis.

Subsequently, the absorption (Ab) and emission (Em) wavelengths of Phi-BTMR probe and Swe-BTR probe were evaluated (Fig. 3A). As expected, the peaks of Ab and Em for Phi-BTMR probe were 542 and 578 nm, respectively, and those for the Swe-

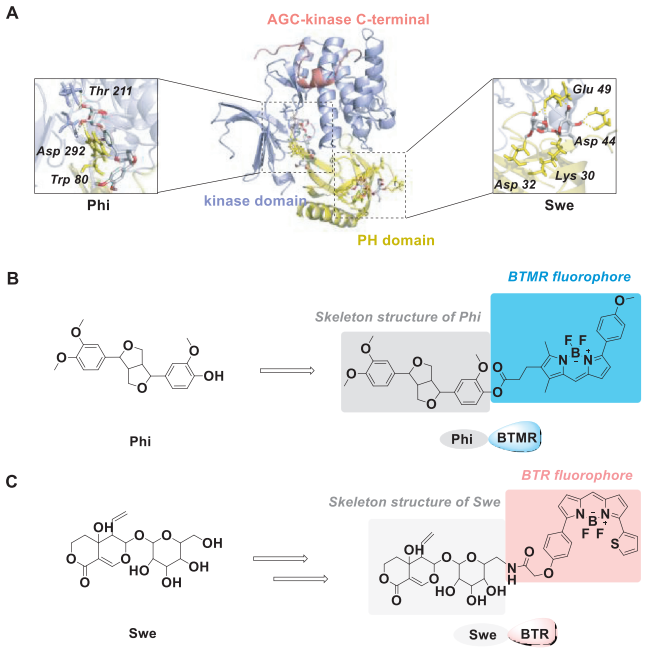

Fig. 2. The FRET analysis preparations of Phi and Swe. (A) Molecular modeling of AKT with Phi and Swe. PyMOL software was used to display the 3D maps of the interactions of AKT with Phi and Swe in the allosteric inhibit pocket and PH domain, respectively. (B) The structures of Phi and the Phi-BTMR probe. (C) The structures of Swe and the Swe-BTR probe.

BTR probe were 606 and 636 nm, respectively. The fluorescence quantum yields of the two fluorescent substances detected by fluorescence spectrophotometer is 0.81 and 0.76, respectively, indicating that both Phi-BTMR probe and Swe-BTR probe have strong fluorescence [25,26]. Due to the desirable overlap of the wavelength spectrum between the Em of Phi-BTMR and the Ab of Swe-BTR (approximately 550–650 nm), which suggested the probes could be applied to FRET analysis. Then, the photoexcitation energy of donor Phi-BTMR was set at 514 nm, and the acceptor of Swe-BTR probe was set at 620–670 nm (Fig. 3B). To test the feasibility of the FRET method, BEAS-2B cells were exposed to an environment containing Phi-BTMR, Swe-BTR and combination probes. The results are shown in Fig. 3C, under excitation at 514 nm, only Phi-BTMR showed *pseudo* blue fluorescence and partially merged with the AKT protein (*pseudo* cyan). In the combination group, the *pseudo* red fluorescence of Swe-BTR was clearly observed, which mainly colocalized with Phi-BTMR (*pseudo* purple) and partially merged with the AKT protein (*pseudo* yellow) on the cell membrane and cytoplasm. The results indicated that Phi and Swe could concurrently bind with the AKT protein at different domains at the cellular level.

In the inactive and active states of AKT, the structural features are diverse [27]. The combination of 5 μmol/L Phi and 20 μmol/L Swe significantly inhibited the Ser473 phosphorylation of AKT, and the activation state of AKT^{S473} was driven by an intramolecular structural transformation between the C-tail and the PH domain linker [28]. Hence, the structural stability of AKT in the inactive state was further analyzed. In cellular thermal shift assay (CETSA), AKT protein denatured with increasing gradient temperature. Compared to the control (Con), Phi or Swe group, AKT protein degeneration was observably inhibited in the combination group at 61 and 64 °C (Figs. 4A and B). Moreover, the combination significantly improved the stability of AKT protein and decreased the digested AKT protein in the drug affinity responsive target stability (DARTS) analysis (Figs. 4C and D). The results suggested that the combination of 5 μmol/L Phi and 20 μmol/L Swe was able to increase the structural stability of AKT in an inactive state at the cellular level.

To demonstrate that Swe and Phi can concurrently work on AKT with different domains *in vivo*, Phi-BTMR and Swe-BTR probes were administered to mice *via* intraperitoneal injection. As shown in Fig. 5A, the fluorescence of Phi-BTMR probe (*pseudo* blue)

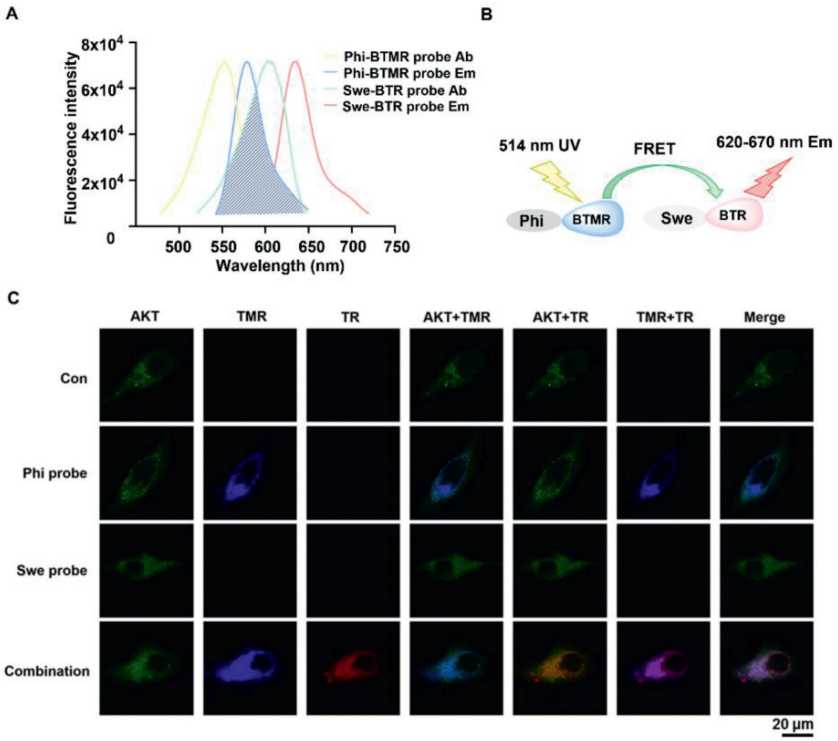

Fig. 3. FRET analysis of the combination of Phi and Swe in cells. (A) Ab and Em wavelength detection of Phi-BTMR probe and Swe-BTR probe. (B) The process of fluorescent energy transfers in FRET analysis. (C) The fluorescent localization of AKT protein (*pseudo* green), Phi-BTMR probe (*pseudo* blue) and Swe-BTR probe (*pseudo* red) in BEAS-2B cells.

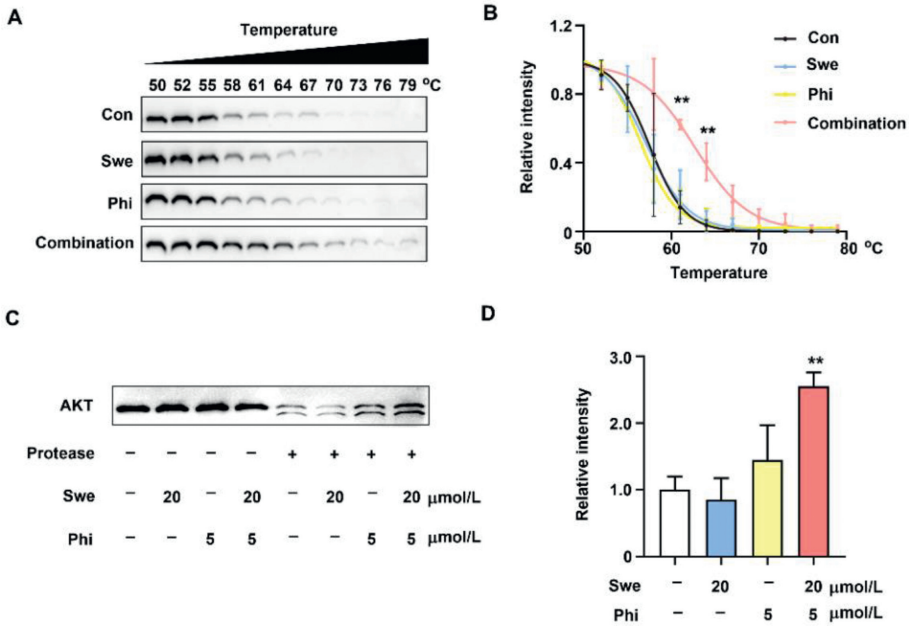

Fig. 4. BEAS-2B cells were pretreated with or without 5 µmol/L Phi, 20 µmol/L Swe or the combination of 5 µmol/L Phi and 20 µmol/L Swe. CETSA was detected by Western blot (A), and the relative intensity of total AKT is presented as the mean ± SD of three experiments (B). DARTS analysis was performed by Western blot (C), and the relative intensity of total AKT with protease to total AKT without protease in each group is presented as the mean ± SD of three experiments (D). $^{**}P < 0.01$ compared to the control group (Con).

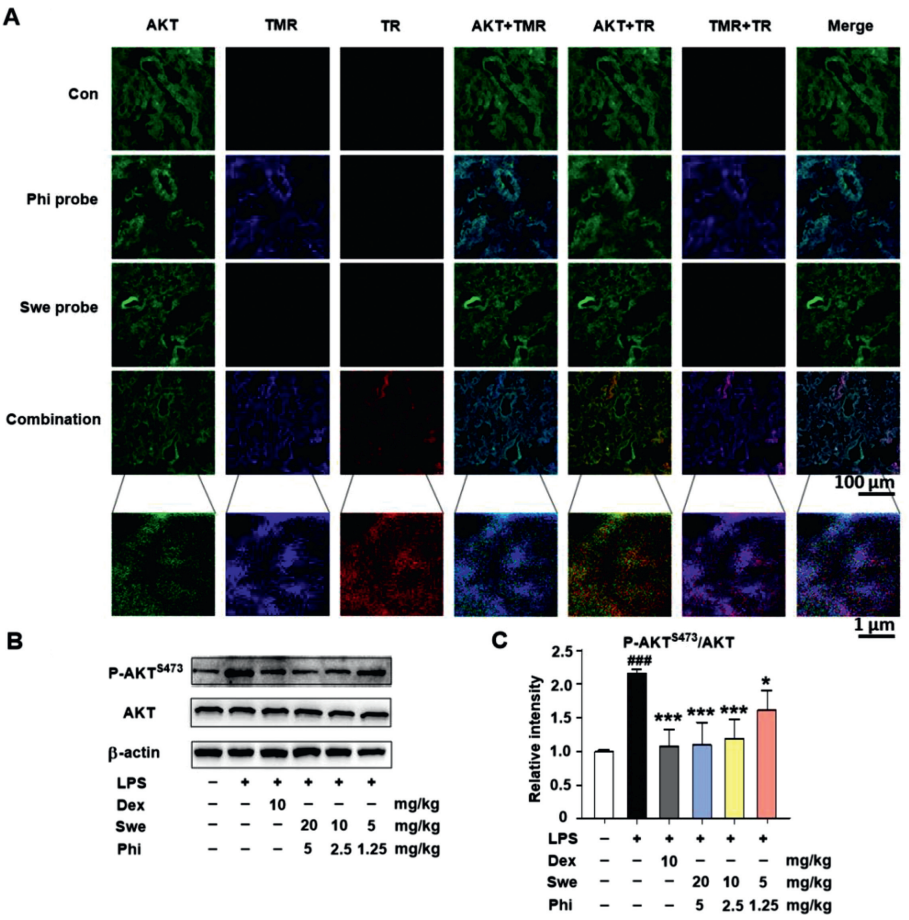

Fig. 5. FRET analysis of the combination of Phi and Swe *in vivo*. (A) The fluorescent localization of AKT protein (*pseudo* green), Phi-BTMR probe (*pseudo* blue) and Swe-BTR probe (*pseudo* red) in lung tissue. The mice were pretreated with different combination doses of Phi and Swe for 6 h, and then stimulated with 10 mg/kg LPS for 90 min. The activation of AKT was detected by Western blot (B), and the relative intensity of P-AKT^{S473} to that of total AKT is presented as the mean ± SD of three experiments (C). $^{###}P < 0.001$ compared to the control group; $^{*}P < 0.05$, $^{***}P < 0.001$ compared to the model group (LPS group).

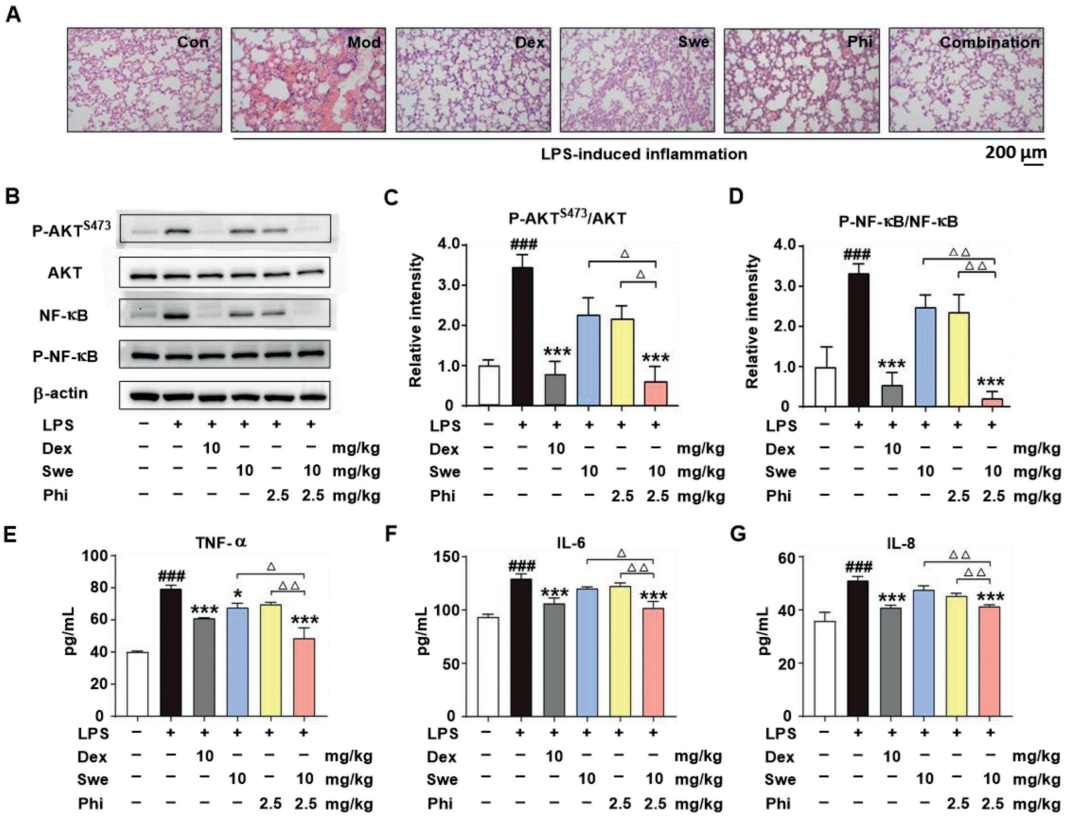

Fig. 6. Anti-inflammatory effect analysis of the combination of Phi and Swe *in vivo*. The mice were pretreated with Phi, Swe or the combination of Phi and Swe for 6 h, and then stimulated with 10 mg/kg LPS for 90 min. (A) Histopathological changes in the lung tissue observed by hematoxylin and Eosin (H&E) staining. Scale bar: 200 μm. (B) The phosphorylation of AKT and NF-κB was detected by Western blot. The relative intensity assay of P-AKT^{S473}/AKT (C) and P-NF-κB/NF-κB (D) ($n = 3$). The contents of TNF-α (E), IL-6 (F) and IL-8 (G) in BALF were measured by enzyme linked immunosorbent assay (ELISA) kits ($n = 6$). $^{\#\#\#}P < 0.001$ compared to the control group (Con); $^{*}P < 0.05$, $^{***}P < 0.001$ compared to the model group (LPS group); $^{\Delta}P < 0.05$, $^{\Delta\Delta}P < 0.01$ compared to the combination group (Swe plus Phi).

partially colocalized with AKT (*pseudo* green) both in the Phi-BTMR group and the combination group, which merged and shown *pseudo* cyan. As expected, the fluorescence Ab of Swe-BTR was dependent on the Em of Phi-BTMR for FRET analysis. Hence, the fluorescence of Swe-BTR probe (*pseudo* red), which was observed only in the combination group, mainly colocalized with the Phi-BTMR probe (*pseudo* purple) and partially merged with the AKT protein (*pseudo* yellow). In addition, the fluorescence of Phi-BTMR probe, Swe-BTR probe and AKT protein were also partially merged together in lung sections.

Next, to evaluate the combination effect in LPS-induced inflammatory mice, the phosphorylation levels of AKT were detected on different combinations of Phi and Swe. The group treated with 2.5 mg/kg Phi and 10 mg/kg Swe exerted a better effect than the group treated with 1.25 mg/kg Phi and 5 mg/kg Swe, and showed a similar effect as the combination of 5 mg/kg Phi and 20 mg/kg Swe (Figs. 5B and C).

To evaluate the anti-inflammatory effect of combination administration *in vivo*, LPS-induced lung inflammation was examined. Histologically, LPS stimulation caused capillary congestion and inflammatory cell infiltrates in lung tissue, which were compared to the Con group. Meanwhile, treatment with Phi, Swe or the combination of Phi and Swe obviously alleviated lung injury and decreased the inflammatory infiltrate in small airways (Fig. 6A). Then, the activation of AKT and downstream inflammatory proteins, NF-κB, in the lung lysates was measured. As shown in Figs. 6B–D, LPS-induced phosphorylation of AKT and NF-κB was significantly increased, and activation was markedly decreased by the combination of 2.5 mg/kg Phi and 10 mg/kg Swe. Compared to the Phi and Swe groups, the inhibition effect of the combination group was observably enhanced on the phosphorylated activation of AKT and NF-κB. Then, the cytokine levels of tumor necrosis factor-α (TNF-α), interleukin (IL)-6 and IL-8 in broncho alveolar lavage fluid (BALF) were further detected. As shown in Figs. 6E–G, only 10 mg/kg Swe reduced the expression of TNF-α. However, the combination of Phi and Swe markedly reduced the expressions of TNF-α, IL-6 and IL-8 in BALF, which exerted a better anti-inflammatory effect compared to the Phi group and Swe group. The above results suggested that the combination of Phi and Swe significantly increased the inhibitory effect on AKT activity and the anti-inflammatory effect.

Pharmacological investigations into combination effects can be examined at the level of the molecular targets, disease pathways, cellular processes, and patient responses [29]. As such, *in vitro*, *in vivo*, preclinical, and clinical research can all provide valuable insight into combination effects [30]. Understanding how mixtures work in combination to exert the biological effect may enhance insight into pharmacological research of natural products or address the ever-increasing threat of disease resistance [31]. In our study, the combination of 5 μmol/L Phi and 20 μmol/L Swe significantly enhanced the inhibitory effect on AKT activity and the anti-inflammatory effect *in vitro*. Integrated with the animal research of LPS-induced inflammation, Phi and Swe concurrently bound with the different domains of AKT and were considered the potential mechanism by which the combination of Phi and Swe alleviated inflammation.

FRET-based fluorescent probes are beneficial in illuminating the underlying pathophysiological mechanism at the molecular scale and provide clear insights into the interactions of proteins or molecules with proteins [32,33]. AKT, a multi domain protein,

contains the N-terminal PH domain followed by an unstructured linker, a protein kinase domain, and a flexible C-terminal AGC-kinase domain. In our study, the fluorescence efficiency of Phi-BTMR probe could excite the Swe-BTR probe, which suggested that the donor and acceptor pair were positioned in proximity to each other (typically 10–100 Å). Combined with the results of molecular docking and previous studies [14,15], we illustrated that Phi and Swe both concurrently acted on the AKT protein at different binding pockets both *in vitro* and *in vivo*.

It is known that the activation of AKT is able to phosphorylate the inhibitor of kappa B kinase (IKK)/NF-κB complex and plays a key role in the activation of NF-κB, which is critical for the expression of inflammatory cytokines, such as IL-6 and IL-8 [34,35]. In the absence of stimulus signals, AKT is autoinhibited, with the PH domain interacting with the kinase domain in a closed conformation [36]. The C-terminal AGC-kinase domain interacts with the PH domain, which relieves PH domain-mediated AKT autoinhibition in the phosphorylation of Ser473 activation [37]. Moreover, the allosteric inhibit pocket is at the interface of the protein kinase domain and the PH domain of the inactive conformation of AKT, and the allosteric inhibitor is able to stabilize the closed conformation by the target allosteric inhibit pocket [38]. As we known, the activation of AKT is directly related to its intramolecular interaction and structural transformation [27]. In the CETSA and DARTS analysis, the combination markedly stabilized the structure of AKT protein in an inactive state. The result indicated that Swe acted on the PH domain to enhance AKT autoinhibition and Phi bond to the allosteric inhibit pocket to stabilize the closed conformation of AKT, which synergistically stabilized the inactive state of AKT.

In the classical model of AKT regulation, AKT is recruited to the plasma membrane by phospholipid phosphatidyl inositol 3,4,5-triphosphate (PIP3), and Ser473 is phosphorylated by 3-phosphoinositide-dependent protein kinase 1 (PDPK1) [39]. The PIP3 molecule binds to the PH domain and allosterically activates AKT, and the PH domain inhibitor influences PIP3 binding in cells [28]. Moreover, the allosteric inhibitor of AKT kinase inhibits the interaction with PDPK1 and facilitates the impairment of AKT signaling downstream [40]. The combination of Swe and Phi targeted the PH domain and the allosteric inhibit pocket to increase the inactive conformation stability of AKT and weaken the response of AKT to LPS stimulation in the PDPK1/AKT signaling pathway, which induced a reduction in NF-κB activation and inflammatory cytokine expression.

The allosteric inhibit pocket provides high specific inhibition and minimal off-target pharmacology in the AKT structure [41]. Compared to traditional competitive inhibitors, allosteric inhibitors have the potential to overcome mutation-associated drug resistance [42]. Therefore, allosteric inhibitors are always used in combinatorial drug therapy, such as perifosine, an allosteric inhibitor of AKT, combined with 5-FU to promote the anticancer effect in colon cancer cells with PIK3CA mutations [43]. In our study, Phi allosterically inhibited AKT, and Swe induced the autoinhibition of AKT. The combined utilization markedly enhanced the inhibitory effect on the activation of AKT and the anti-inflammatory activity both *in vitro* and *in vivo*.

In this paper, we found that Phi and Swe concurrently targeted AKT on different domains by FRET. Phi and Swe, in combination, enhanced the structural stability of AKT in an inactive state, reduced phosphorylated activation, and inhibited the inflammatory response.

Declaration of competing interest

The authors declare that they have no known competing financial interests or personal relationships that could have appeared to influence the work reported in this paper.

Acknowledgment

This research was supported by the National Natural Science Foundation of China (No. 81973449).

Supplementary materials

Supplementary material associated with this article can be found, in the online version, at doi:10.1016/j.cclet.2023.108823.

References

[1] Y. Wang, Q. Xie, H.D. Tan, et al., Pharmacol. Res. 173 (2021) 105702.
[2] S. Gomez, T. Tabernacki, J. Kobyra, et al., Cancer Biol. 65 (2020) 99–113.
[3] A. Huttner, J. Bielicki, M.N. Clements, et al., Clin. Microbiol. Infect. 26 (2020) 871–879.
[4] L. Xu, X.Y. Cui, J.B. Liao, et al., Chin. Chem. Lett. 33 (2022) 3701–3704.
[5] W.Y. Zhang, J. Gao, C.J. Cheng, et al., Cancers 12 (2020) 311.
[6] J.T. Hwang, J. Ha, I.J. Park, et al., Cancer Lett. 247 (2007) 115–121.
[7] G. Chevereau, T. Bollenbach, Mol. Syst. Biol. 11 (2015) 807.
[8] J. Tang, K. Wennerberg, T. Aittokallio, Front. Pharmacol. 6 (2015) 181.
[9] N.C. Kaneider, B. Mosheimer, N. Reinisch, et al., Thromb. Res. 114 (2004) 185–194.
[10] X. Chen, L. Qian, B.J. Wang, et al., Molecules 24 (2019) 955.
[11] L.J. Zhang, C. Virgous, H.W. Si, J. Nutr. Biochem. 69 (2019) 19–30.
[12] X.Y. Leong, P.V. Thanikachalam, M. Pandey, et al., Biomed. Pharmacother. 84 (2016) 1051–1060.
[13] Z.Y. Wang, Q. Xia, X. Liu, et al., J. Ethnopharmacol. 210 (2018) 318–339.
[14] M. Zhang, X.Y. Ma, H.L. Xu, et al., FEBS J. 287 (2020) 1816–1829.
[15] W.J. Liu, G.C. Chu, N.W. Chang, et al., RSC Adv. 7 (2017) 40418–40426.
[16] Y.S. Sun, H. Wallrabe, S.A. Seo, et al., ChemPhysChem 12 (2011) 462–474.
[17] X.J. Zhang, Y. Hu, X.T. Yang, et al., Biosens. Bioelectron. 138 (2019) 111314.
[18] X.T. Shen, W. Xu, J. Ouyang, et al., Chin. Chem. Lett. 33 (2022) 4505–4516.
[19] P. Jia, Y. Hu, Z. Zeng, et al., Chin. Chem. Lett. 34 (2023) 107511.
[20] D. Wu, A.C. Sedgwick, T. Gunnlaugsson, et al., Soc. Rev. 46 (2017) 7105–7123.
[21] Y. Xu, C. Li, J. An, et al., Sci. China Chem. 66 (2023) 155–163.
[22] L. Wu, C.S. Huang, B.P. Emery, et al., Chem. Soc. Rev. 49 (2020) 5110–5139.
[23] M. Gangopadhyay, R. Mengji, A. Paul, et al., Chem. Commun. 53 (2017) 9109–9112.
[24] S. Chen, Y.L. Yu, Encycl. Anal. Sci. 2019 (2019) 341–348.
[25] A.M. Brouwer, Pure Appl. Chem. 83 (2011) 2213–2228.
[26] W. Zhai, Y. Zhang, M. Liu, et al., Angew. Chem. Int. Ed. 58 (2019) 16601–16609.
[27] C.C. Kumar, V. Madison, Oncogene 24 (2005) 7493–7501.
[28] M. Ebner, I. Lučić, T.A. Leonard, et al., Mol. Cell. 65 (2017) 416–431.
[29] T. Pemovska, J.W. Bigenzahn, G. Superti-Furga, Curr. Opin. Pharmacol. 42 (2018) 102–110.
[30] H. Wagner, G. Ulrich-Merzenich, Phytomedicine 6 (2009) 97–110.
[31] T. Efferth, E. Koch, Curr. Drug Targets 12 (2011) 122–132.
[32] J. Yoo, J.Y. Kim, J.M. Louis, et al., Nat. Commun. 11 (2020) 3336.
[33] N. Ojha, K.H. Rainey, G.H. Patterson, Nat. Commun. 11 (2020) 21.
[34] Y.H. Fan, R.F. Mao, J. Yang, Protein Cell 4 (2013) 176–185.
[35] D. Bai, L. Ueno, P.K. Vogt, Int. J. Cancer 125 (2009) 2863–2870.
[36] V. Calleja, M. Laguerre, P.J. Parker, et al., PLoS Biol. 7 (2009) e17.
[37] N. Chu, A.L. Salguero, A.Z. Liu, et al., Cell 174 (2018) 897–907.
[38] L. Quambusch, I. Landel, L. Depta, et al., Angew. Chem. Int. Ed. 58 (2019) 18823–18829.
[39] D.D. Sarbassov, D.A. Guertin, S.M. Ali, et al., Science 307 (2005) 1098–1101.
[40] A.E. Leroux, J.O. Schulze, R.M. Biondi, Semin. Cancer Biol. 48 (2018) 1–17.
[41] Z.Z. Fang, C. Grütter, D. Rauh, ACS Chem. Biol. 8 (2013) 58–70.
[42] D.L. Gibbons, S. Pricl, H. Kantarjian, et al., Cancer 118 (2012) 293–299.
[43] Y. Morii, M. Tsubaki, T. Takeda, et al., Eur. J. Pharmacol. 898 (2021) 173957.